Journal of Research of the National Bureau of Standards—A. Physics and Chemistry
Vol. 68A, No. 2, March–April 1964

Polymorphism of Bismuth Sesquioxide. II. Effect of Oxide Additions on the Polymorphism of Bi_2O_3

Ernest M. Levin and Robert S. Roth

The effect of small oxide additions on the polymorphism of Bi_2O_3 was studied by means of high-temperature x-ray diffractometry. Solidus and occasional liquidus temperatures were approximated, so that tentative partial phase diagrams for 33 oxide additions were constructed. Only the monoclinic and the cubic forms of Bi_2O_3 were found to be stable. Other phases, frequently reported by previous investigators, such as tetragonal and body-centered cubic (b.c.c.), were shown to form metastably from cooled liquid or cubic. An impure b.c.c. phase of distinct but variable composition appeared in systems of ZnO, PbO, B_2O_3, Al_2O_3, Ga_2O_3, Fe_2O_3, SiO_2, GeO_2, TiO_2, and P_2O_5. The impure b.c.c. phase in the systems with SiO_2, GeO_2, and TiO_2 melted congruently about 100 °C above the m.p. of Bi_2O_3. The impure b.c.c. phase was formed metastably in systems with Rb_2O, NiO, MnO, CdO, V_2O_5, and Nb_2O_5; the conditions of formation were dependent on composition, preparation, and heating schedules. The impure b.c.c. phases, both stable and metastable, had smaller unit cell dimensions than that of pure Bi_2O_3.

1. Introduction

Part I of this paper was an attempt to clarify the stable and metastable relationships of pure Bi_2O_3. It can be seen in table 1 of that part, however, that several investigators [1,2,3] [1] have reported phases of Bi_2O_3 which contained, or were contaminated by, other oxides. Sillén [1] obtained a body centered cubic (b.c.c.) form by fusing Bi_2O_3 in porcelain, or with Al_2O_3 or Fe_2O_3, for 5 min at 900 °C. He suggested the unit cell formula $Me_2Bi_{24}O_{40}$. Fusion of Bi_2O_3 in a porcelain crucible for 20 min yielded cubic Bi_2O_3. Schumb and Rittner [2] also obtained the impure b.c.c. phase by fusing Bi_2O_3 at 875 °C in porcelain or with SiO_2. By quenching the fused mixture in water, they produced an impure cubic (C) phase. Gattow and Schröder [3] reported impurity forms of b.c.c., C, and tetragonal-symmetry, designated respectively, as γ^*, δ^*, β^*.

The previous work can be questioned on two grounds: Firstly, in most cases the exact compositions were not controlled and were not known; secondly, in no instances were the phases studied at temperature and, consequently, might not represent stable equilibrium phases. Quenched liquids, for example, could hardly be expected to give equilibrium phases for any temperature. Furthermore, as the stable phases of Bi_2O_3 have been shown to be monoclinic and cubic-bismuth oxide, any other phase, e.g., impure tetragonal (Tet) or b.c.c. must represent either a metastable form of Bi_2O_3 or a discrete phase, whose composition limits does not include Bi_2O_3.

The major objective of this portion of the study, therefore, was to obtain information on the impure forms of bismuth oxide, in particular, on the b.c.c. phase. To eliminate objections applicable to previous work, mixtures were formulated from pure materials and of known compositions and were studied in a high-temperature x-ray diffractometer furnace.

[1] Figures in brackets indicate the literature references at the end of this paper.

2. Materials and Methods

2.1. Materials

For the admixture study, reagent grade chemicals (ACS) or those of higher purity were used. Starting materials for formulating oxide mixtures with Bi_2O_3 were as follows: Li_2CO_3, Rb_2CO_3, NiO, ZnO, CdO, MgO, $CaCO_3$, $SrCO_3$, $BaCO_3$, PbO, B_2O_3, Al_2O_3, Ga_2O_3, Fe_2O_3, $MnCO_3$, Sb_2O_3, Lu_2O_3, Sm_2O_3, La_2O_3, SiO_2, GeO_2, TiO_2, TeO_2, SnO_2, ZrO_2, CeO_2, P_2O_5, V_2O_5, Sb_2O_5, Ta_2O_5, Nb_2O_5, Cr_2O_3, WO_3, and MoO_3. These materials were chosen from crystal chemistry considerations, such as charge, ionic radius, coordination number, and polarizability of the cations.

2.2. Preparation of Mixtures

Binary mixtures were formulated from Bi_2O_3 and a second substance, to give an atomic ratio in most cases of 12Bi to 1Me, where Me represents the second cation. The intent was to determine which oxides formed Sillén's [1] impure b.c.c. phase at the above ratio. Thus for monovalent, trivalent, and pentavalent cations, oxide compositions would correspond to $12Bi_2O_3$:Me_2O, $12Bi_2O_3$:Me_2O_3, and $12Bi_2O_3$:Me_2O_5. For divalent, tetravalent, and hexavalent cations, oxide compositions would correspond to $6Bi_2O_3$:MeO, $6Bi_2O_3$:MeO_2, and $6Bi_2O_3$:MeO_3. Additional compositions were prepared in many of the systems, as designated on the individual phase diagrams.

Preliminary treatment of the mixtures consisted of three cycles of grinding together calculated amounts of the starting materials, pressing the material in a mold, and then heating the disk at a temperature below the solidus, as described in previous publications [4,5].

2.3. Apparatus

The high-temperature, x-ray diffractometer furnace noted in Part I was used also for the admixture study. The modification of the sample holder [6] which permitted the use of a thin layer of powered specimen was of especial importance for this part of the study. X-ray diffraction patterns of crystalline phases could be obtained in the presence of liquid, which did not flow off the platinum holder. Thus, it was possible to approximate solidus temperatures (± 10 °) and under favorable conditions even the liquidus temperatures.

3. Results and Discussion

3.1. Phase Diagrams

a. General Remarks

The data obtained by use of the high-temperature x-ray furnace can be presented in the form of phase diagrams, as shown in figures 1 through 6. Arrangement of the figures is according to the Periodic Table. Within each figure, diagrams are arranged, in general, according to a combination of the Periodic Table subgroups and ionic radii of the atoms. As no table of data is given, figure captions include selected notes. In most instances, the rate of disappearance of old phases and of the appearance of new ones on the indicated boundary curves was not rapid but took place over a temperature interval. Phases which have been interpreted as nonequilibrium ones are not shown in the diagrams.

It is emphasized that these phase diagrams represent the best interpretation of the data within the limitations of the experimental method. The major limitation is due to volatility of the samples or of the constituents. The high surface-to-volume ratio inherent with a thin film method, increases the effect of volatilization on composition. Thus, verification of equilibrium by long soaking periods, especially at high temperatures, was precluded.

b. General Conclusions

From inspection of all of the diagrams, several general conclusions become evident:

(1) The only stable phases of pure bismuth oxide are Mon and C. The b.c.c. or Tet phases of pure Bi_2O_3 do not appear. The conclusion is consistent with the stability relationships for Bi_2O_3 as deduced in Part I.

(2) Monoclinic Bi_2O_3 shows little or no solid solution.

(3) The C phase of Bi_2O_3, however, may show extensive solid solution; and in such cases, the Mon to C transition temperature is lowered.

(4) Except for the CdO and PbO systems (fig. 2 G& H), the effect of solid solution in the C phase is to raise solidus and liquidus temperatures.

(5) A b.c.c. phase distinct from that of pure Bi_2O_3 appears in a number of systems. This b.c.c. phase may vary in composition for different systems (see figs. 2F, 3B & C, 4A, 5A), may melt congruently (fig. 4A, B & C), or melt incongruently (figs. 2H, 3A & B), and when stable is separated from Bi_2O_3 by a two-phase region.

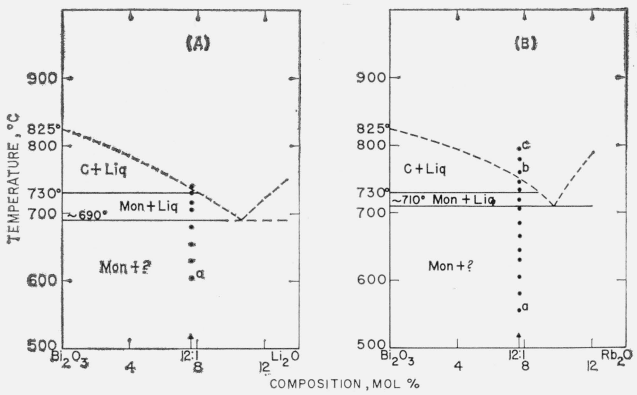

FIGURE 1. Bi_2O_3 *rich regions of* $Bi_2O_3-R_2O$ *systems, as determined from high-temperature x-ray diffraction data.*

Phases: Mon—monoclinic, C—cubic, ?—unknown, Liq—liquid
(A) $Bi_2O_3-Li_2O$
a—Trace of unknown phase observed.
(B) $Bi_2O_3-Rb_2O$
a—No second phase seen.
b—Rb_2O apparently volatilizes from liquid.
c—Liquid cools to b.c.c. phase: a=10.22A.

c. Individual Phase Diagrams

In the following section, individual figures and selected diagrams will be discussed. Only two alkali oxide systems, representing extremes in cation radii, were studied (fig. 1). Both Li_2O and Rb_2O, in the region studied, were simple eutectic types with no solid solutions. It should not be inferred, however, that oxides of the intermediate cations necessarily would behave similarly.

For oxides of the divalent cations (fig. 2) the phase diagrams showed a number of variations, e.g., simple eutectic system (A), congruently melting b.c.c. phase (F), incongruently melting b.c.c. phase (H), C solid solution with liquidus and solidus raised (B), and C solid solution with liquidus and solidus lowered (H).

In the systems with CaO, SrO, and BaO, the rhombohedral solid solution phase described previously [7, 8] was found to be an equilibrium phase. Sillén and Aurivillius had found the phase in samples cooled rapidly from the liquid. The unit cell dimensions at 700 °C for the bismuth oxide-rich compositions of the solid solution phase are given in table 1.

Sillén and Sillén [9] report finding several phases in the Bi_2O_3-CdO system, one of which might be the

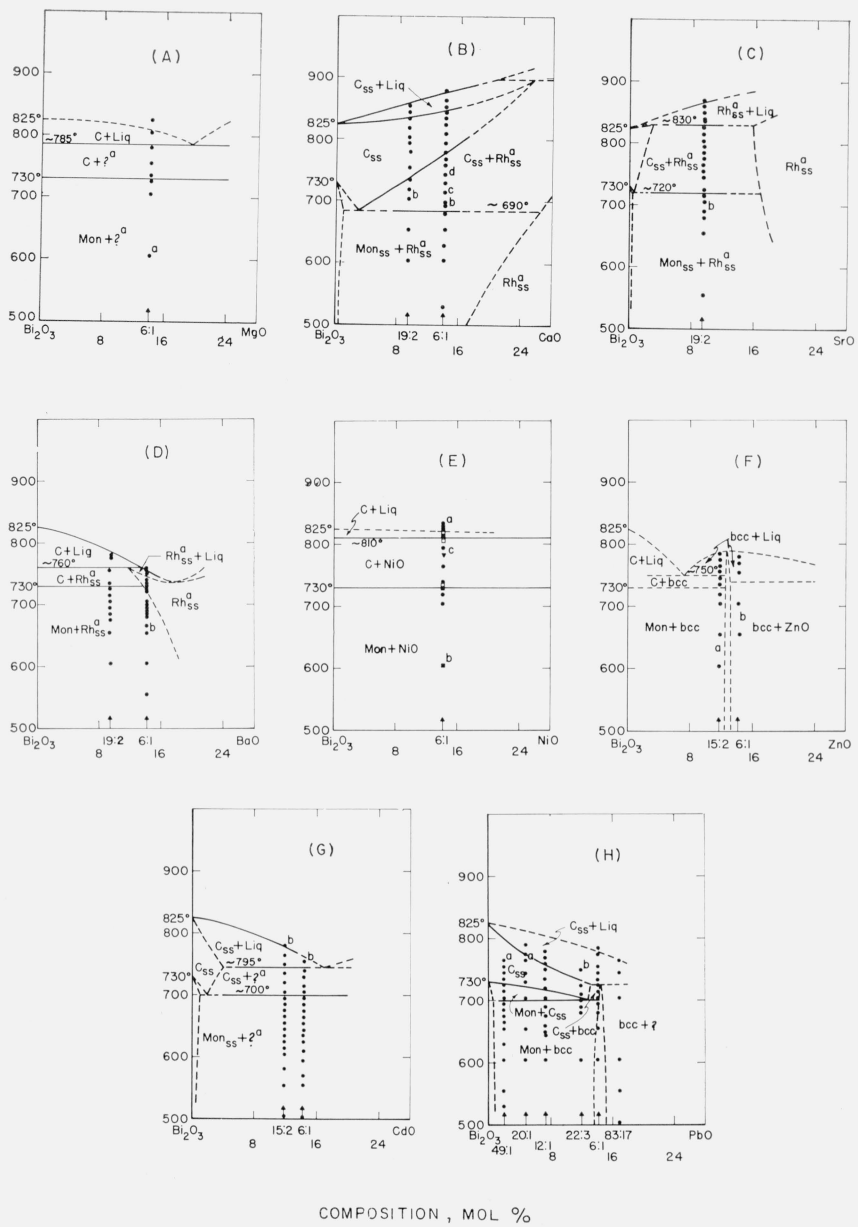

FIGURE 2. Bi_2O_3 *rich regions of* Bi_2O_3-RO *systems, as determined from high-temperature x-ray diffraction data.*

Phases: Mon—monoclinic, C—cubic, b.c.c.—body-centered cubic, ?—unknown, Rh—rhombohedral, ss—solid solution, Liq—liquid

(A) Bi_2O_3—MgO
a—Second phase, possibly MgO.

(B) Bi_2O_3—CaO
a—Described by Aurivillius (1943) [7].
b—Cubic Bi_2O_3 ss starting to form.
c—Cubic Bi_2O_3 ss increasing; Mon Bi_2O_3 decreasing.
d—Mon Bi_2O_3 gone.
The 6:1 composition slow-cooled from 700 °C (after 107 hr soaking period) shows single phase Rh_{ss}. See table 1 for unit cell dimensions.

(C) Bi_2O_3—SrO
a—Described by Sillén and Aurivillius (1939) [8].
b—Rh_{ss} increasing; Mon decreasing. See table 1 for unit cell dimensions.

(D) Bi_2O_3—BaO
a—Described by Aurivillius (1943) [7].
b—Rh_{ss} increasing; Mon decreasing. See table 1 for unit cell dimensions.

(E) Bi_2O_3—NiO
a—Liq cools to b.c.c.
●—First heat
□—b.c.c. reheated
■—Superposition of ● and □.
▼—Reheated sample cooled from liq to 780 °C
b—b.c.c. decomposing to Mon.
c—Cubic phase when cooled to room temperature shows b.c.c.

(F) Bi_2O_3—ZnO
a—No Mon detected.
b—ZnO detected only in specimen soaked 107 hr at 700 °C and then slow-cooled.
The two compositions studied indicate that the b.c.c. phase is stable and melts congruently. Beyond this the diagram is conjectural.

(G) Bi_2O_3—CdO
a—Possibly one of Sillén's reported $CdO-Bi_2O_3$ phases [9].
b—Liq cools to b.c.c.

(H) Bi_2O_3—PbO
a—C_{ss} cools to b.c.c.
b—C_{ss}+ Liq cools to b.c.c.

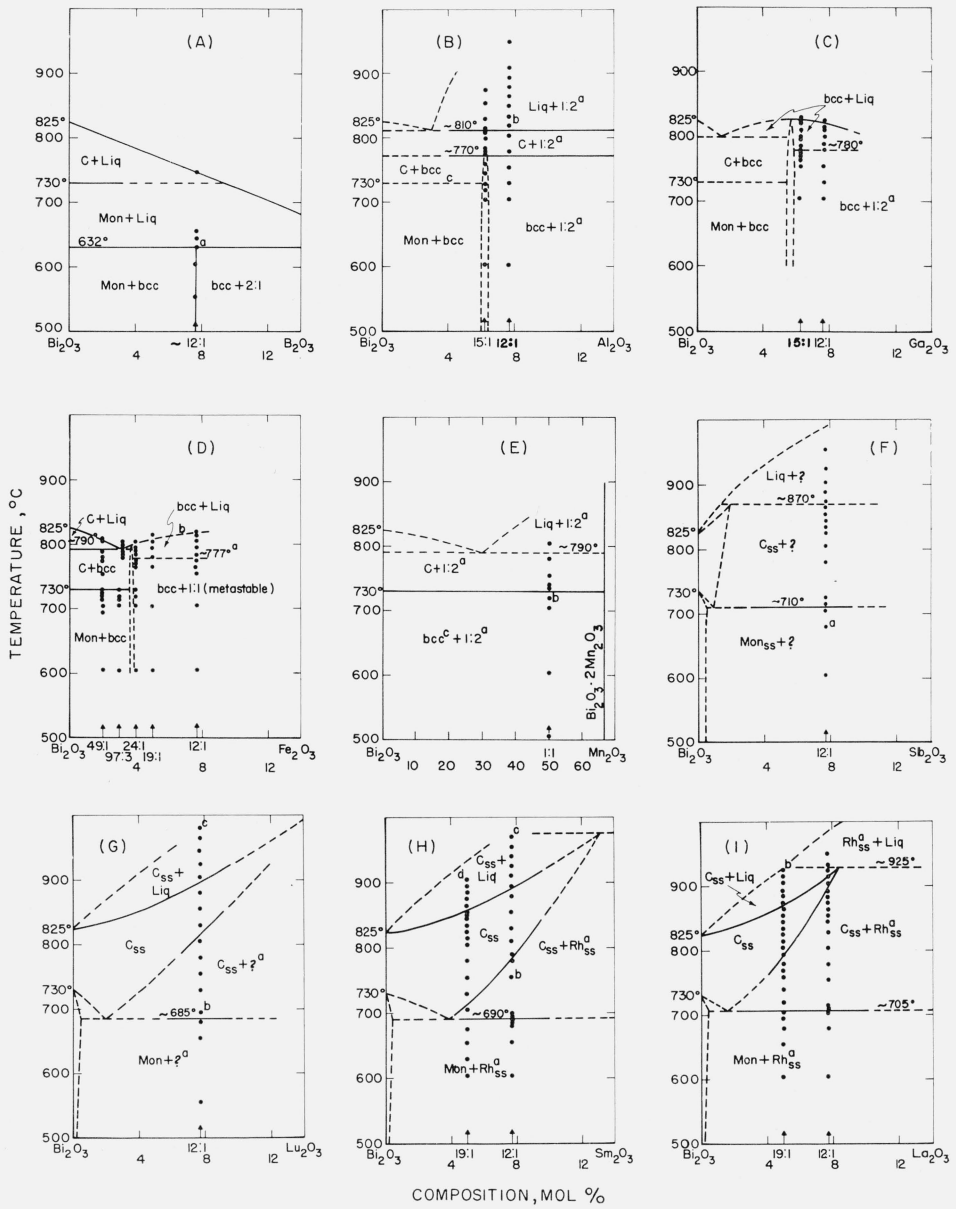

FIGURE 3. Bi_2O_3 *rich regions of* $Bi_2O_3-R_2O_3$ *systems, as determined from high-temperature x-ray diffraction data.*

Phases: Mon—monoclinic, C—cubic, b.c.c.—body-centered cubic, ?—unknown, Rh—rhombohedral, ss—solid solution, Liq—liquid.

(A) $Bi_2O_3-B_2O_3$
Diagram taken from Levin et al. [4].
a—Unreacted $2Bi_2O_3 \cdot B_2O_3$(2:1) and Mon Bi_2O_3 at lower temperatures form single phase b.c.c.

B) $Bi_2O_3-Al_2O_3$
a—Isostructural with 1:2 compounds in systems of Bi_2O_3 with Fe_2O_3, Ga_2O_3, and Mn_2O_3, according to unpublished work of R. S. Roth.
b—Very strong peak at *d* value about 2.9A; probably orientation of $Bi_2O_3 \cdot 2Al_2O_3$.
c—Effect of Al_2O_3 on Mon to C transition temperature not determined.

(C) $Bi_2O_3-Ga_2O_3$
a—Isostructural with 1:2 compounds in systems of Bi_2O_3 with Fe_2O_3, Al_2O_3, Mn_2O_3, according to unpublished work of R. S. Roth.
The two compositions studied indicate that the b.c.c. phase is stable and melts congruently. Beyond this the diagram is conjectural.

(D) $Bi_2O_3-Fe_2O_3$ (Does not obey phase rule.)
a—May represent metastable eutectic between b.c.c. and metastable $BiFeO_3$.
b—Liquidus curve does not show maximum temperature at melting of b.c.c. phase.
The $BiFeO_3$ phase is believed to be metastable because the compound composition can never be made single phase, according to the unpublished work of R. S. Roth.

(E) $Bi_2O_3-Mn_2O_3$ (Note different composition scale.) $MnCO_3$ used as starting material, and mixture ground in alcohol, which tends to give b.c.c.[17].
a—Isostructural with 1:2 compounds in systems of Bi_2O_3 with Fe_2O_3, Al_2O_3, Ga_2O_3, according to unpublished work of R. S. Roth.
b—Samples at this temperature and below show b.c.c., believed to be metastable, as it disappears at Mon to C inversion (730 °C).
c—Mon Bi_2O_3 probably stable phase (see b).

(F) $Bi_2O_3-Sb_2O_3$
a—Above about 650 °C oxidation state of the antimony is unknown. Starting with Sb_2O_5, same phases occur, but solidus appears to be lower (~855 °C).

(G) $Bi_2O_3-Lu_2O_3$
a—Second phase observed, with major *d* value at 2.95A.
b—As Mon transorms to C, unreacted Lu_2O_3 transforms to ? phase.
c—Liq+C_{ss} cools to metastable tetragonal$_{ss}$.

(H) $Bi_2O_3-Sm_2O_3$
a—Essentially isostructural with Rh_{ss} phase in CaO—, SrO—, and BaO—Bi_2O_3 systems. See table 1 for unit cell dimensions.
b—When cooled to 450 °C shows Rh_{ss}+ tetragonal (Tet)$_{ss}$ (metastable).
c—Liq+C_{ss} cools to Tet_{ss}+C_{ss} (both metastable).
d—Liq+C_{ss} cools to Tet_{ss} (metastable). Single phase Tet_{ss} (19:1) reheated to 625 °C transforms first to C_{ss}+Rh_{ss}, then the C_{ss} transforms to the equilibrium Mon phase.

(I) $Bi_2O_3-La_2O_3$
a—Essentially isostructural with Rh_{ss} phase in CaO—, SrO—, and BaO—Bi_2O_3 systems. See table 1 for unit cell dimensions.
b—Cools to C_{ss} (metastable)

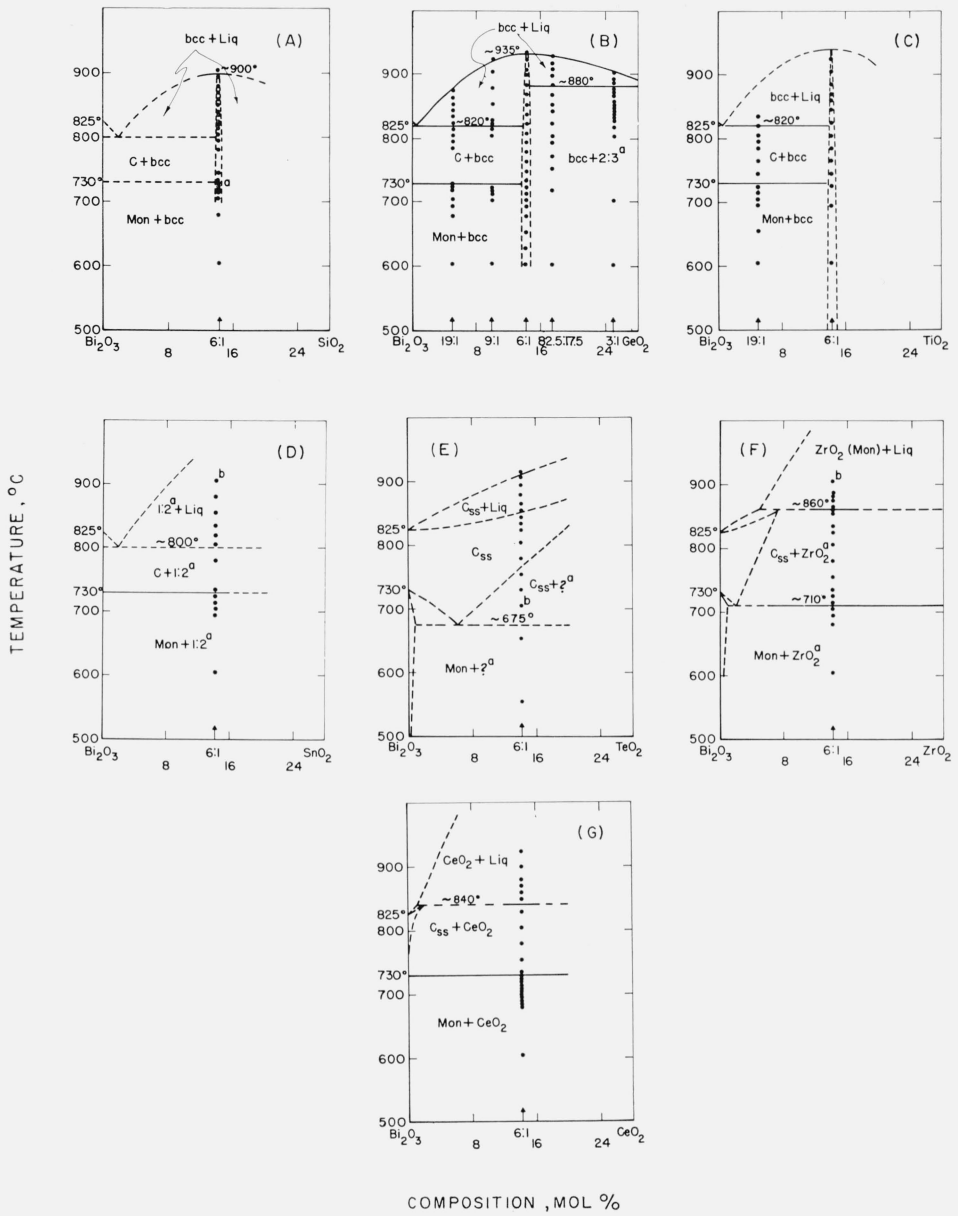

FIGURE 4. Bi_2O_3 *rich regions of* $Bi_2O_3-RO_2$ *systems, as determined from high-temperature x-ray diffraction data.*

Phases: Mon—monoclinic, C—cubic, b.c.c.—body-centered cubic, ?—unknown, ss—solid solution, Liq—liquid

(A) $Bi_2O_3-SiO_2$
a—Unreacted Mon transforms to C, on heating.
Composition studied shows that the b.c.c. phase (6:1) melts congruently. Beyond this the diagram is conjectural.

(B) $Bi_2O_3-GeO_2$
a—Unpublished work of C. R. Robbins, NBS.
Compositions studied show that the b.c.c. phase melts congruently, near to but not necessarily at the 6:1 composition.

(C) $Bi_2O_3-TiO_2$
Compositions studied show that the b.c.c. phase melts congruently, near to but not necessarily at the 6:1 composition.

(D) $Bi_2O_3-SnO_2$
a—Compound described by R. S. Roth [14].
b—1:2 + Liq cools to 1:2 + Mon + b.c.c. (trace).

(E) $Bi_2O_3-TeO_2$
Oxidation state of tellurium at high temperature is unknown.
a—Unknown composition, apparently of cubic symmetry.
b—Unit cell dimensions at 700 °C: C_{ss}, a=5.63A; ?, a=5.57A

(F) $Bi_2O_3-ZrO_2$
a—ZrO_2 does not show in x-ray pattern below solidus.
b—Liq + ZrO_2 (Mon) cools to Tet Bi_2O_{3ss}.
No b.c.c. found in this system although reported by Aurivillius and Sillén [15].

(G) $Bi_2O_3-CeO_2$
No b.c.c. found in this system although reported by Aurivillius and Sillén [15].

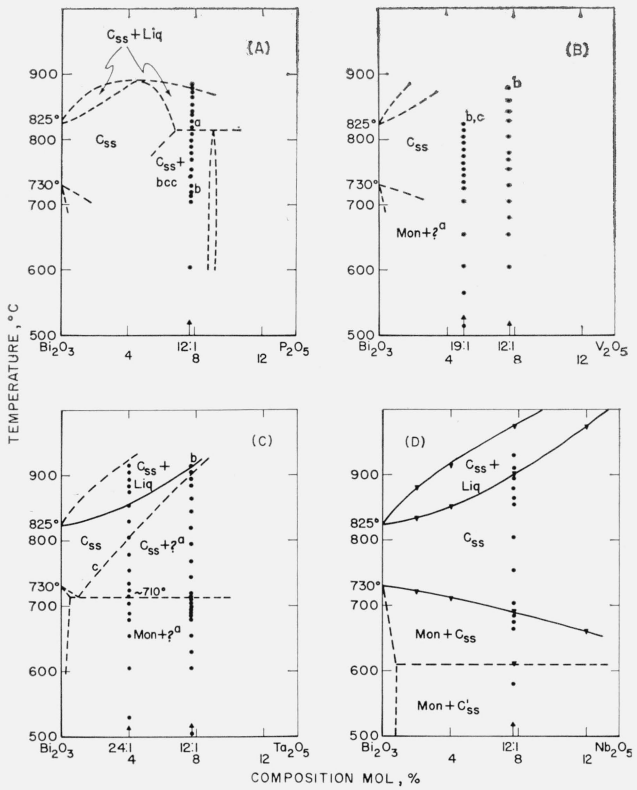

FIGURE 5. Bi_2O_3 *rich regions of* $Bi_2O_3-R_2O_5$ *systems, as determined from high-temperature x-ray diffraction data.*

Phases: Mon—monoclinic, C—cubic, C′—pseudocubic, b.c.c.—body-centered cubic, ?—unknown, ss—solid solution, Liq—liquid

(A) $Bi_2O_3-P_2O_5$
- a—The b.c.c. phase decreases markedly in amount at about 815 °C, but persists in diminishing amounts to about 850 °C. It is possible, therefore, that the true solidus is at 850 °C and (1) a 2-phase region of C_{ss} + ? exists between 815 ° and 850 °C or (2) the decomposition temp. of b.c.c. should be raised to 850 °C.
- b—The Mon to C transition with the high-temp. x ray occurs at about 720 °C. However, a sample held at 700 °C for 107 hr and slow-cooled does not show Mon. Therefore, the temperature of the Mon to C inversion is in doubt.

(B) $Bi_2O_3-V_2O_5$

A more complete phase diagram could not be postulated because of inconsistencies in the temperatures of transitions and the relative amounts of phases present.
- a—b.c.c., if a stable phase; otherwise, unknown phase.
- b—Above 815 °, only C_{ss}; between 715 ° and 815 °C, C_{ss} + b.c.c.; below 715 °C, phases present depend on previous heat treatment. Stability and approximate composition of b.c.c. could not be ascertained.
- c—C_{ss} cools to b.c.c.

(C) $Bi_2O_3-Ta_2O_5$
- a—Apparently cubic symmetry; composition may correspond to C′ phase in $Bi_2O_3-Nb_2O_5$ system [17] (about 4:1).
- b—Liq + C_{ss} cooled slowly shows only C_{ss} at all temps.
- c—Because of nonreversibility (see b), this boundary may actually be much lower, as in the $Bi_2O_3-Nb_2O_5$ system (D).

(D) $Bi_2O_3-Nb_2O_5$

▼—Values taken from phase diagram of Roth and Waring [17].

unknown phase in the present study of the cadmium oxide system (fig. 2G).

The PbO-Bi_2O_3 system (fig. 2H) is interesting for several reasons. It varies significantly from the reported phase diagram of Belladen [10, 11]. The latter shows neither the Mon to C transition, nor the solid solution of PbO in Bi_2O_3, nor the b.c.c. phase at the $6Bi_2O_3$·PbO composition. It is evident from the present diagram that the molal heat of fusion of Bi_2O_3 calculated by Kelley [12] from the liquidus curve of Belladen's diagram (6800 cal/mole) is in error. The molal heat of fusion of Bi_2O_3 was discussed by Levin and McDaniel [4].

With regard to the systems of bismuth oxide with oxides of the trivalent cations, the Bi_2O_3-B_2O_3 system (fig. 3A) was reported previously [4], as determined by the quenching technique. However, one composition, $12Bi_2O_3:B_2O_3$, was used to compare both methods and to show that agreement was satisfactory.

Apparently isostructural 1:2 compounds were found in systems of Bi_2O_3 with Al_2O_3 (fig. 3B), Ga_2O_3 (fig. 3C), and Mn_2O_3 (fig. 3E). An isostructural 1:2 compound also exists in the Bi_2O_3–Fe_2O_3 system; however, the high-temperature x-ray study revealed only a 1:1 compound (fig. 3D). The

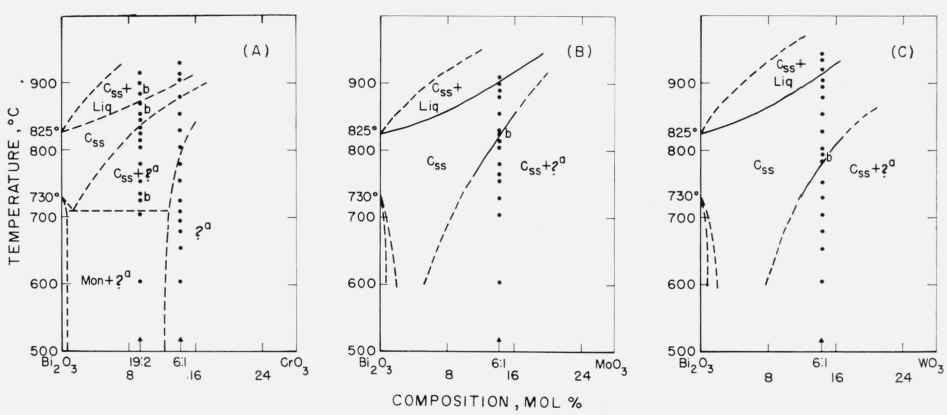

FIGURE 6. Bi_2O_3 *rich regions of* $Bi_2O_3-RO_3$ *systems, as determined from high-temperature x-ray diffraction data.*

Phases: Mon—monoclinic, C—cubic, ss—solid solution, ?—unknown, Liq—liquid

(A) $Bi_2O_3-CrO_3$

Compositions formulated from Cr_2O_3. Diagram shown on CrO_3 basis because on calcining, specimens changed in color from green to red, and ? phase is similar to that formed with the hexavalent ions.
- a—Unknown composition, apparently pseudotetragonal (similar to the phase in the $Bi_2O_3-MoO_3$ and $Bi_2O_3-WO_3$ systems).
- b—Phases found at these temps. do not agree entirely with postulated phase boundaries, because system may be pseudobinary.

(B) $Bi_2O_3-MoO_3$
- a—Unknown composition, apparently pseudotetragonal (similar to the phase in the $Bi_2O_3-CrO_3$ and $Bi_2O_3-WO_3$ systems).
- b—Reversibility demonstrated with high-temp. x ray.

(C) $Bi_2O_3-WO_3$
- a—Unknown composition, apparently pseudotetragonal (similar to the phase in the $Bi_2O_3-CrO_3$ and $Bi_2O_3-MoO_3$ systems).
- b—Reversibility demonstrated with high-temp. x ray.

TABLE 1. *Unit cell demensions of rhombohedral phases formed in* Bi_2O_3 *systems*

Oxide addition	Starting composition	Final heat treatment	Additional phases present	Ionic radius of cation (Ahrens)	Unit cell dimensions				
					Hexagonal			Rhombohedral	
		°C/hr			a A	c A	c/a	a A	α
CaO [a]	$6Bi_2O_3$:CaO	700°/107	None	0.99	3.94_1	27.9_5	7.09	9.59_0	23°44′
SrO [a,b]	$19Bi_2O_3$:2SrO	699°/144	Mon Bi_2O_3 (moderate)	1.12	3.95_2	28.0_9	7.11	9.63_7	23°40′
BaO [a]	$6Bi_2O_3$:BaO	700°/107	b.c.c. Bi_2O_3 (small)	1.34	3.97_2	28.5_4	7.18_5	9.78_6	23°26′
Sm_2O_3	$12Bi_2O_3$:Sm_2O_3	700°/107	tr?	1.00	3.95_0	27.9_3	7.07	9.58_5	23°46′
La_2O_3	$12Bi_2O_3$:La_2O_3	700°/107	b.c.c. Bi_2O_3 (moderate)	1.14	3.97_5	28.1_0	7.07	9.64_4	23°48′

[a] Rhombohedral phase described by Aurivillius [7].
[b] Rhombohedral phase described by Sillén and Aurivillius [8].

$BiFeO_3$ phase is believed to be metastable, because according to the unpublished work of R. S. Roth, the compound composition can never be made single phase. It should also be noted that the portion of the diagram to the right of the b.c.c. phase does not obey the phase rule. Royen and Swars [13] who also have studied this system reported two Tet phases of approximately 30:1 and (12–13):1 compositions, a b.c.c. phase of composition 15:1, as well as 2:1 and 1:1 compounds. The present work does not substantiate the 30:1, (12–13):1, and 2:1 compounds; and the composition of the b.c.c. phase appeared slightly greater than $24Bi_2O_3$:Fe_2O_3. As Royen and Swars obtained their compounds from fused mixtures, it is believed that some of them represented metastable states.

The system with the rare earth oxides Sm_2O_3 (fig. 3H) and La_2O_3 (fig. 3I), showed the same rhombohedral solid solution phase as was found in the CaO, SrO, and BaO systems (fig. 2B–D). The unit cell dimensions are given in table 1. The phase did not form in the Lu_2O_3 system (fig. 3G) nor in the MgO system (fig. 2A); consequently, the minimum cationic radius required for formation of this phase lies between that of Lu^{3+} and Ca^{2+} or between 0.85 and 0.99A (Ahrens).

In the systems studied with the group IV cations (fig. 4), SiO_2 (A), GeO_2 (B), and TiO_2 (C) showed a congruently melting b.c.c. phase at or near the 6:1 composition. The phase diagrams provide positive proof, for the first time, that the impure b.c.c. phase is a discrete composition and not a solid solution phase of Bi_2O_3.

The Bi_2O_3-SnO_2 system (fig. 4D) contains a 1:2 compound described by R. S. Roth [14] as having a distorted pyrochlore-type structure.

No b.c.c. phase was found in the ZrO_2 and CeO_2 systems, although this phase was obtained from fused mixtures by Aurivillius and Sillén [15]. As will be discussed later under the b.c.c. phase, cooling of the liquid or C phases tends to form metastable phases.

In the group V cations (fig. 5), systems with P_2O_5 (A) and V_2O_5 (B) showed inconsistencies which could not be reconciled, and these diagrams are most questionable. The systems with Ta_2O_5 (C) and Nb_2O_5 (D) are similar, and it is possible that the boundary curve in the Ta_2O_5 system between (Css+?) and Css should descend continuously as in the Nb_2O_5 system (see b and c in legend to fig. 5C).

Finally, in the Bi_2O_3–RO_3 systems (fig. 6), the three systems studied are similar, including the occurrence of a phase of apparently pseudotetragonal symmetry but of unknown composition. Gattow [16] prepared a mixed oxide $2Bi_2O_3$·MoO_3, by precipitation from solution, and studied it by means of x-ray and thermal analysis. Because of insufficient data, however, it was not possible to compare the unknown phase in the present study with Gattow's.

3.2. Metastable Phases

The results of the high-temperature x-ray experiments were especially informative regarding the occurrence of metastable phases observed at room temperature in samples cooled from higher temperatures. Such information is included in the figure captions. Illustrative examples are as follows:

(1) Liquid cooled to a metastable b.c.c. phase in Bi_2O_3 systems with Rb_2O (see c to caption of fig. 1B), NiO (a of fig. 2E), and CdO (b of fig. 2G).
(2) Cubic or cubic solid solution cooled to a metastable b.c.c. phase in systems with NiO (c of fig. 2E) and V_2O_5 (c of fig. 5B).
(3) Liquid+cubic solid solution cooled to metastable cubic solid solution in systems with La_2O_3 (b of fig. 3I), Ta_2O_5 (b of fig. 5C), and Nb_2O_5 [17].
(4) Liquid+cubic solid solution also cooled to metastable Tet in systems with Lu_2O_3 (c of fig. 3G), Sm_2O_3 (b and d of fig. 3H), and Nb_2O_5 [17].
(5) In the zirconia system, liquid+ZrO_2 cooled to metastable tetragonal.

It is emphasized that an exhaustive study of the formation of metastable phases was not attempted. In general, only one cooling cycle for a limited number of compositions was studied in each system. It is apparent, however, from the frequency and diversity of the matastable phases found, that phases obtained by the cooling of fused mixtures or of high-temperature forms may well represent nonequilibrium states at all temperatures. It is not surprising, therefore, that previous investigators [1, 2, 13, 15] studying fused samples of unknown compositions obtained various impurity phases. Many of these are metastable phases and have no place in the equilibrium diagrams.

3.3. Body-Centered Cubic Phase

Table 2 gives the unit cell dimensions for the stable and metastable b.c.c. phases of bismuth oxide found in this study. The unit cell dimensions were obtained at room temperature; and except for Rb_2O and Bi_2O_3 (see footnotes d and e, respectively) the samples were heated in sealed platinum tubes according to the schedule given in the column under "Final Heat Treatment". As observed from the x-ray diffraction patterns, most of the compositions studied were not single phase but showed a second phase.

Concerning the systems with a stable b.c.c. phase, it is seen that an exact 12Bi to 1Me atom ratio was not substantiated in most cases. Except for PbO and B_2O_3, systems with divalent and trivalent cations would show single phase b.c.c. at ratios of Bi to Me greater than 12:1. Systems with the tetravalent ions Si^{4+}, Ge^{4+}, and Ti^{4+} approached most closely the ideal ratio of 12Bi:1Me, proposed by Sillén [1]. This conclusion is more apparent from figure 4A,B,C, where the b.c.c. phase in these systems is seen to melt congruently at a temperature about 100 °C above the melting point of Bi_2O_3. With the oxide of the pentavalent cation, P^{5+}, the single phase b.c.c. composition appears to be less than 12Bi:1Me (fig. 5A). It can be seen from table 2 that within each valence group increased ionic radius of the cation is associated with increased unit cell dimensions of the b.c.c. phase. Unit cell dimensions versus ionic radius for all of the cations are plotted in figure 7. The general correlation between the two for the stable phases (solid points) is seen to be good, although not linear.

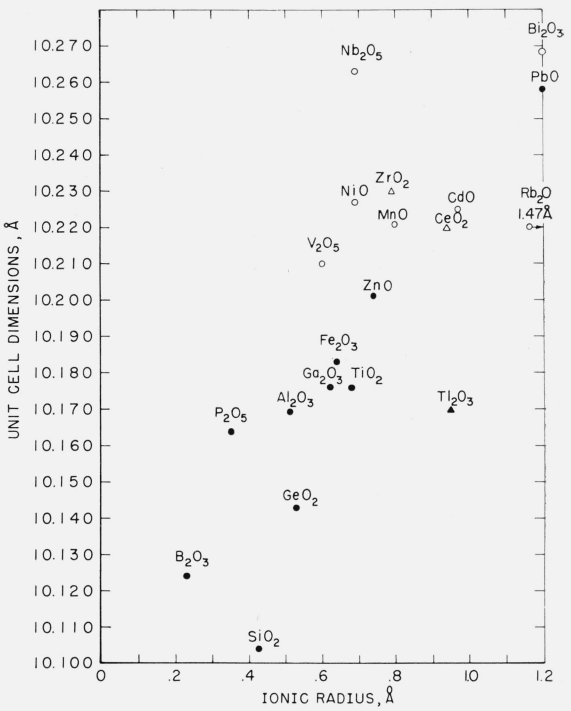

FIGURE 7. *Unit cell dimensions versus ionic radius for impure body-centered cubic phases of* Bi_2O_3.

Oxides shown in the figure refer to the impurity additions. See figures 2 through 5 for approximate compositions of the phases.
●—equilibrium phases
○—metastable phases
▲, △—unit cell dimensions after Aurivillius and Sillén [15].

TABLE 2. *Unit cell dimensions of body-centered cubic phases formed by small additions of oxides to* Bi_2O_3

Oxide addition	Starting composition	Final heat treatment	Additional phases present	Ionic radius of cation (Ahrens)	Levin and Roth	Aurivillius and Sillen [15]
			Stable phases			
		°C/hr		Å	Å	Å [a]
ZnO	$6Bi_2O_3$:ZnO	700°/107	Trace ZnO	0.74	10.20_1	
PbO	$6Bi_2O_3$:PbO	725°/1	None	1.20	10.25_8	10.25 [b]
B_2O_3	$12Bi_2O_3$:B_2O_3	600°/65	Trace Bi_2O_3+ trace 2:1	0.23	10.12_4	
Al_2O_3	$12Bi_2O_3$:Al_2O_3	700°/107	Trace Bi_2O_3·$2Al_2O_3$	.51	10.16_9	10.16
Ga_2O_3	$12Bi_2O_3$:Ga_2O_3	700°/107	Trace Bi_2O_3·$2Ga_2O_3$	.62	10.17_6	
Fe_2O_3	$19Bi_2O_3$:Fe_2O_3 [c]	700°/3	Trace $BiFeO_3$	.64	10.18_3	10.18
Tl_2O_3				.95		10.17
SiO_2	$6Bi_2O_3$:SiO_2	700°/107	Small amt. Bi_2O_3	.42	10.10_4	10.10
GeO_2	$6Bi_2O_3$:GeO_2	700°/107	Trace GeO_2	.53	10.14_3	
TiO_2	$6Bi_2O_3$:TiO_2	700°/107	None	.68	10.17_6	
P_2O_5	$12Bi_2O_3$:P_2O_5	700°/107	Trace?	.35	10.16_4	
			Metastable phases			
Rb_2O	$12Bi_2O_3$:Rb_2O	795°/0.1 [d]	Trace Bi_2O_3	1.47	10.22	
NiO	Bi_2O_3:NiO [c]	785°/1	NiO	0.69	10.22_7	
MnO	Bi_2O_3:MnO [c]	735°/1	Moderate amt. Bi_2O_3·$2Mn_2O_3$	.80	10.22_1	
CdO	$6Bi_2O_3$:CdO	700°/107	Trace CdO	.97	10.22_5	
Bi_2O_3	Bi_2O_3	780°/0.1 [e]	Small amt. Mon Bi_2O_3	1.20 [f]	10.26_8	10.264 [g]
ZrO_2				0.79		10.23
CeO_2				.94		10.22
V_2O_5	$12Bi_2O_3$:V_2O_5	700°/107	Small amt. Tet. Bi_2O_3 ss	.59	10.21_0	
Nb_2O_5	$6Bi_2O_3$:Nb_2O_5 [c]	700°/3	Moderate amt. cubic (C′ [17])	.69	10.19	
Nb_2O_5	$24Bi_2O_3$:Nb_2O_5 [c]	700°/3	Trace cubic (C′ [17])	.69	10.26_3	

[a] Converted from kx units.
[b] Cation is tetravalent according to Aurivillius and Sillen [15].
[c] Starting materials ground together in alcohol.
[d] Sample cooled from liq. in high-temp., x-ray furnace.
[e] Slow-cooled in high-temp., x-ray furnace.
[f] Ahrens gives 0.96Å, which is low. See [4].
[g] Agrees with value obtained by Schumb & Rittner [2].

An interesting and surprising finding is that oxides of cations so diverse in ionic radius, oxygen coordination number, and polarizability as Zn^{2+}, B^{3+}, Ti^{4+}, and Pb^{2+} can form with bismuth oxide a discrete phase of the same symmetry. An appealing explanation is the concept of a clathrate- or cage-type structure, in which as postulated by Sillén [1] for $Si_2Bi_{24}O_{40}$, central Si atoms are surrounded by spheres of $Bi_{12}O_{20}$ atoms. For the case of a central ion with valence different from 4, charge balance would be achieved through cation or oxygen adjustments.

Regarding the metastable b.c.c. phase, the monovalent ion Rb^+ formed the phase on cooling in the high temperature x-ray experiments. The compositions containing NiO, MnO, and Nb_2O_5, which in the process of preparation were ground in alcohol, also formed the b.c.c. phase, metastably. These results would seem to support the conclusion that an impure b.c.c. phase of Bi_2O_3 might be formed (metastably) with most cations, under the proper conditions of composition, grinding, and heating schedules.

It is seen from figure 7 that with the exception of PbO the unit cell dimensions of the metastable phases are larger than those of the stable phases. The cell dimensions of the metastable impure phases, also, are less than those for the b.c.c. metastable phase of pure Bi_2O_3. Therefore, the compositions of the impure metastable phases cannot be that of pure Bi_2O_3. However, contrary to the case of the stable b.c.c. phases, no correlation exists between unit cell dimensions and ionic radius for the metastable b.c.c. phases. The x-ray diffraction patterns of the b.c.c. phases of the stable and metastable impurity forms are similar in d spacings and intensities to the pattern for pure Bi_2O_3. It is a reasonable assumption that the structures are similar.

To summarize (see fig. 7), the b.c.c. phase of pure Bi_2O_3 has the largest unit cell dimensions, and the addition of a foreign ion to Bi_2O_3 tends to decrease the dimensions. This decrease is least for the larger ions, which tend to form the metastable b.c.c. phase. The decrease in cell dimensions is greatest for the smaller ions, which tend to form the stable b.c.c. phase. Whereas the stable b.c.c. phases show correlation with ionic radius, the metastable phases do not. These findings are compatible with a cage-type structure in which a central cation, including Bi, is surrounded by a sphere of atoms of approximately $Bi_{12}O_{20}$ composition.

4. Summary

The important phase equilibria relationships for the bismuth-rich portions of the phase diagrams are shown schematically in figure 8. Elements in boldfaced type refer to the respective oxide mixtures studied. Elements enclosed in heavy outlines represent oxides which formed the stable b.c.c. phase with bismuth oxide. Composition of the b.c.c. phase was found to be variable for different systems, but most nearly approached the ideal 12Bi:1Me ratio for oxides of the tetravalent ions Si^{4+}, Ti^{4+}, and Ge^{4+}. Designations in the upper right-hand corners of the boxes for the stable b.c.c. phases refer to the nature of melting, e.g., congruent, incongruent, or decomposition. Oxides of elements which formed the metastable b.c.c. phase are indicated by an *M* in the upper right-hand corner of the box, and those that formed the rhombohedral solid solution phase, by *Rh*. The nature of the liquidus curves is indicated by a designation in the lower right-hand corner of each box, as follows: *E*, simple eutectic; ss_r, solid solution type with liquidus and solidus raised; ss_L, solid solution type with liquidus and solidus lowered.

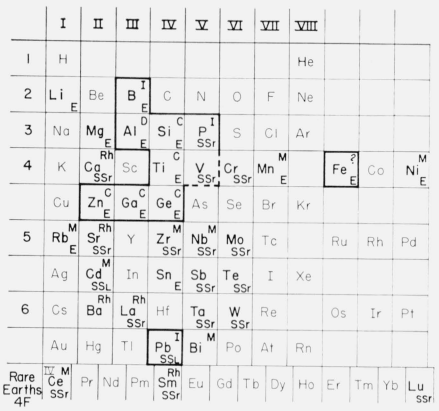

FIGURE 8. *Summary of some phase equilibria data on the effect of oxide additions to* Bi_2O_3. *Elements shown in boldfaced type on the Periodic Table refer to oxide additions.*

Elements enclosed in heavy outlines represent oxides which form stable body-centered cubic phases with bismuth oxide:
C—congruently melting
I—incongruently melting
D—decomposes
M—metastable body-centered cubic phase
E—eutectic-type system
SS_r—solid solution of oxide in Bi_2O_3, with solidus and liquidus raised
SS_L—solid solution, with solidus and liquidus lowered
Rh—rhombohedral solid solution phase [7, 8].

The authors acknowledge their sincere appreciation to Robert Friedman, who as a guest worker, summer 1961, from the University of Chicago, prepared the compositions and obtained some of the unit cell dimensions.

5. References

[1] L. G. Sillén, Arkiv fr Kemi, Mineral. Geol. **12A** [18] 1–13 (1937).
[2] W. C. Schumb and E. S. Rittner, J. Am. Chem. Soc. **65,** 1055–1060 (1943).
[3] G. Gattow and H. Schröder, Z. anorg. u allgem. Chem. **318** [3–4] 176–189 (1962).
[4] E. M. Levin and C. L. McDaniel, J. Am. Ceram. Soc. **45** [8] 355–360 (1962)
[5] E. M. Levin, C. R. Robbins, and J. L. Waring, J. Am. Ceram. Soc. **44** [2] 87–91 (1961).

[6] E. M. Levin and F. A. Mauer, J. Am. Ceram. Soc. **46** [1] 59–60 (1963).
[7] B. Aurivillius, Arkiv. Kemi, Mineral. Geol. **16A,** No. 17, 1–13 (1943).
[8] L. G. Sillén and B. Aurivillius, Z. Krist. **101,** 483–495 (1939).
[9] L. G. Sillén and B. Sillén, Z. Phys. Chem. **B49,** 27–33 (1944).
[10] L. Belladen, Gazz. chim. ital. **52II,** 160–164 (1922).
[11] See also, E. M. Levin, H. F. McMurdie, and F. P. Hall "Phase Diagrams for Ceramists", The American Ceramic Soc., Inc., fig. 97, p 58 (1956).
[12] K. K. Kelley, U.S. Bur. Mines Bull., No. 393, 166 pp (1936); p 26; Ceram. Absts., **16** [5] 162 (1937).
[13] P. Royen and K. Swars, Angew. Chem. **69** [24] 779 (1957).
[14] R. S. Roth, J. Research NBS **56** [1] 17–25 (1956); RP 2643.
[15] B. Aurivillius and L. G. Sillén, Nature **155,** No. 3932, 305–306 (1945).
[16] G. Gattow, Z. anorg. Chem. **298,** 65–71 (1959)
[17] R. S. Roth and J. L. Waring, J. Research NBS **66A** [6] 451–463 (1962).

(Paper 68A 2–269)